ELSEVIER

Journal of Molecular Catalysis A: Chemical 166 (2001) 135–145

JOURNAL OF MOLECULAR CATALYSIS A: CHEMICAL

www.elsevier.com/locate/molcata

Methane partial oxidation in iron zeolites: theory versus experiment

P.P. Knops-Gerrits [a,b,*], W.A. Goddard III [b,1]

[a] *Laboratory of Inorganic Chemistry and Organic Materials (CMAT), Chemistry Department, Université Catholique de Louvain (UCL), Lavoisier Building, Place L. Pasteur no. 1, B-1348, Louvain-la-Neuve, Belgium*

[b] *Material and Process Simulation Center, Beckman Institute (139-74), California Institute of Technology, Pasadena CA91125, USA*

Received 3 February 2000; received in revised form 7 March 2000; accepted 24 March 2000

Abstract

The conversion of methane to methanol over zeolitic α-oxygen sites has been demonstrated using Fe-ZSM-5. To discriminate between mono- and poly-nuclear active sites, we prepared the [Fe]-ZEO with iron in the ZEOlite lattice via direct synthesis and Fe_x-ZEO, by dispersion of *x* wt.% iron on the ZEOlite. Shape-selective formation of nano-clusters of iron oxides with various sizes is realized inside the pore-sizes varying from 10.0 to 8.0 and 6.3 to 4.3 Å of the CFI, MOR, MFI, and CHA zeolites. The Fe–K edge X-ray absorption data were obtained for the Fe-CIT-5, Fe-ZSM-5, Fe-MOR and Fe-CHA zeolites containing iron clusters. In Mossbauer spectroscopy the absence and presence of a hyperfine magnetic field (HMF) for [Fe]-CIT-5 and Fe-CIT-5 are seen. The quantum mechanics calculations analyze the different environments of iron, e.g. the tetrahedral lattice occluded species, the di-nuclear sites attached to the zeolite, the nano-phase hematite sites. The molecular mechanics calculations involve a new molecular mechanics force field, the universal force field (UFF). α-Oxygen can be formed on di-nuclear iron sites in zeolites by N_2O decomposition at elevated temperatures and is dependent on the zeolite structure utilized. Fe-chabazite (CHA), Fe-mordenite (MOR) and Fe-CIT-5 (CFI) were found to be less active than Fe-ZSM-5. A range of preparative and activation conditions were studied preceding methane conversion. Proper activation is essential to maximize catalyst actvity, e.g. pretreatment under vacuum at 800–900°C, activation with N_2O at 250°C and reaction with methane at 20°C. Extraction of methanol from the catalyst is performed with H_2O. Structure–activity effects are discussed.

Keywords: Iron zeolites; Methane conversion; Zeolite synthesis; Metal nuclearity; ab initio calculation; Force field; Physico-chemical characterisation

1. Introduction

Direct methane conversion to useful chemical products has long been the holy grail of catalytic science, however, numerous approaches have so far failed to overcome the severe thermodynamic barriers associated with this reaction [1–10]. Some recent papers by Panov et al. describe the methane activation on so-called α-oxygen sites that are formed on iron sites on Fe-ZSM-5 [1–3] by N_2O decomposition at elevated temperature [4,5]. Such materials are also used as catalysts for the conversion of benzene into phenol [11–24]. This reaction was commercialized, using the N_2O being produced in an adjacent adipic acid plant [18,19]. A formal inverse correlation between

* Corresponding author. Present address: Département de Chimie, Université Catholique de Louvain (UCL), Batiment Lavoisier, Place L. Pasteur no. 1, B-1348 Louvain-la-Neuve, Belgium. Tel.: +32-1047-4045; fax: +32-1047-2836.

E-mail addresses: ppkg@chim.ucl.ac.be (P.P. Knops-Gerrits), wag@wag.caltech.edu (W.A. Goddard III).

[1] Tel.: +1-626-395-2731; fax: +1-626-585-0918.

1381-1169/01/$ – see front matter
PII: S1381-1169(00)00460-X

the Bronsted acid site concentration and the oxidation rate is observed in this reaction. The activation of benzene employs an acid mechanism and H-ZSM-5 catalysts [14–25], this of methane employs a redox mechanism and Fe-ZSM-5 catalysts [1–3]. In N_2O decomposition mono- and bi-molecular routes exist depending on pressure and temperature. In situ Mossbauer studies implicate the reduction of Fe^{III} to Fe^{II} in the stoichiometric reaction by N_2O decomposition on these catalysts [1]. Fe-ZSM-5 is more active than a Ga-ZSM-5 type catalyst [20–21]. For benzene conversion, substituting Al by Fe is to be avoided since the isomorphous substituted system at a SiO_2/M_xO_y of 90 gave an inferior selectivity of 90 versus 98% at 16% conversion [23–27]. We previously studied extensively by which mechanism di-nuclear iron clusters are active in the alkane activation [33,34]. In this work evaluation of Fe-ZSM-5 and other Fe zeolite systems in order to optimize methane conversion activity. A new 14 MR material CIT-5 (CFI) [6], is functionalized with iron. Mono-nuclear iron sites in [Fe]-ZSM-5, di-nuclear iron clusters stabilized inside the matrix of thermally activated Fe-ZSM-5 and iron sites associated with various other zeolites are compared using theoretical tools as well as experiments.

2. Experimental

The zeolites are made from basic silicate solution with organic templates. Low molecular weight silicate species such as Cab-O-Sil M5 (Cabot Corporation) or LUDOX HS 30 (DuPont), $Fe(NO_3)_3$ salt (Aldrich) and $Fe^{III}(acac)_2$ complex (Aldrich) and $Al(NO_3)_3$ salt (JT-Baker) are used as silicate, iron and aluminum precursors, LiOH or NaOH are added. The basic silicate solution can be added to an acidified ferric salt solution, to give an overall basic gel. The acidified ferric salt solution contains O-coordination complexes such as nitrates or acetylacetonates of iron. These form stable complexes at low pH, but slowly dissociate in a basic medium liberating the metal ions. During the dissociation the silica can bind to form the ferri-silicate gel thus, avoiding the precipitation of iron as hydroxides. Once the ferri-silicate gel is formed, precipitation of iron is avoided even at higher pH. The organic structure directing agents are 1-adamanteinium-trimethyl-ammonium-hydroxide (ATMA, CHA), tetra-ethyl-ammonium-bromide (TEABr, mordenite), tetra-propyl-ammonium-bromide (TPABr, ZSM-5), *N*(16)-methyl-sparteinium-hydroxide (NMSP-OH, CIT-5). Iron is introduced in zeolite lattices via direct synthesis. Zeolites are synthesized hydrothermally in a temperature range of 423–448 K. The syntheses are carried out in sealed quartz tubes (75 mm × 15 mm i.d.) and in Teflon-lined Parr reaction vessels.

2.1. [Fe]-CHA

The gel contains the LUDOX HS-40 silica, Catapal Al, $Fe(NO_3)_3$ and LiOH and ATMAOH is added as the SDA. A mixture with following stoichiometry ATMAOH (4.5 g):4 K_2O (11.22 g):Al_2O_3 (1.35 g):0.1 $Fe(NO_3)_3$ (1.28 g):8 SiO_2 (30.05 g):200 H_2O (16.5 g) is heated at 100°C at autogeneous pressure for 7 days to form Fe-CHA (Si/Fe = 80).

2.2. [Fe]-ZSM-5

The gel contains $Fe(NO_3)_3$ acidified with sulfuric acid, LUDOX HS-30 silica and TPABr is added as the SDA. The mixture with following stoichiometry is heated at 150°C at autogeneous pressure for 6 days form ZSM-5 (Si/Fe = 68):2.4 TPABr (1.2 g):13 NaOH (1 g):$Fe(NO_3)_3$ (0.75 g):68 SiO_2 (2.211 g):4 H_2SO_4 (0.75 g):1000 H_2O (16.5 g). A ZSM-5 support is prepared analogously, with following stoichiometry: 2 TPABr (0.98 g):2 NaOH (0.29 g):20 SiO_2 (2.21 g):500 H_2O (16.5 g).

2.3. [Fe]-MOR

The gel contains LUDOX HS-30 silica, $Fe(NO_3)_3$ acidified with sulfuric acid, and the SDA TEABr. The mixture with following stoichiometry is heated at 175°C at autogeneous pressure for 2 days to form Fe-MOR:2 TEABr (1.0 g):22 NaOH (0.29 g):0.33 $Fe(NO_3)_3$ (0.460 g):20 SiO_2 (2.211 g):4 H_2SO_4 (0.75 g):450 H_2O (15.0 g).

2.4. [Fe]-CIT-5

The gel contains either $Al(NO_3)_3$ and $Fe(acac)_3$ to which LiOH as the mineralizer and LUDOX HS-30 is added and the SDA. A reaction mixture with following composition is heated at 175°C at autogeneous pres-

sure for 12 days to produce Al-CIT-5:0.2 MeSPAOH (1.27 g):0.1 LiOH (0.18 g):0.02 Al_2O_3 (1.50 g):1 SiO_2 (2.10 g):40 H_2O (3.47 g). A second synthesis mixture with composition: 0.2 MeSPAOH (1.27 g):0.1 LiOH (0.18 g):0.02 $Fe(acac)_2$ (0.06 g):1 SiO_2 (2.10 g):40 H_2O (3.47 g) is heated at 175°C at autogeneous pressure for approximately 7 days and yields Fe-CIT-5. The recovered solid is washed with distilled, deionized water, and allowed to air dry. Either LiOH (Fisher) alone, or a mixture of LiOH together with either NaOH (Aldrich) or KOH (Aldrich) can be used, CIT-5 can be formed in the absence of Li^+ cations if the alkali cation (K^+ or Na^+) is present in very low concentration. ([ROH]/[SiO_2] less than 0.05) while the total [OH^-]/[SiO_2] ratio is held constant at 0.3. The gel requires SDA *N*(16)-methyl-sparteinium hydroxide (**I**) (MeSPAOH), and LiOH to form CIT-5, as in absence of LiOH, the product is SSZ-24 (silica analog of $AlPO_4$-5). Pure silica CIT-5 can be prepared in 5 days, as Al or Fe are introduced in a synthesis mixture, synthesis times increase.

Iron is also dispersed by solid state exchange on zeolites. Commercial samples of ZSM-5 (VAW Company, Si/Al ∼ 11), MOR (TOSOH, Si/Al ∼ 10), CHA (PQ Company, Si/Al ∼ 4) were obtained and a sample of CIT-5 was prepared according to a procedure reported [6]. Prior to their use the samples are calcined at 550°C. The solid state exchange occurs after a calcination at 550°C under O_2 by temperature programmed heating at 1°C/min to 175°C, 2 h at 175°C, at 1°C/min to 550°C and 4–8 h at 550°C. The amount of $Fe^{III}(acac)_2$ mixed with zeolites is varied to obtain an iron loading of ∼5, ∼2.5, ∼1.25 and ∼0.5%, respectively.

Catalytic oxidation of methane with N_2O is carried out in a specially designed quartz cell that is linked to a vacuum line. The quartz cell is contained within an oven. A catalyst sample (0.5–1.0 g, particles with a mesh size of 35–60) is loaded in the quartz cell. The sample occupies a negligible volume compared to the total reaction volume of the unit (210 cm^3), this to allow accurate adsorption of the gas phases. Extractions are performed on the samples in glass vials and with variety of solutions, e.g. acetonitrile-water or pure H_2O or D_2O. The products are analyzed by GCMS on a HP-FFAP column. As a standard a solution of methanol in acetonitrile in GCMS analysis shows presence of both and a mixture of the species with mass fragments H_3COCH_2 55, CHCN 41, CH_2CN 42 and CH_3CN 43, HCO 29, due to hydrolysis of acetonitrile.

3. Results and discussion

3.1. Formation and characterization of new materials

The introduction of iron into the lattice of zeolites such as CFI MFI, MOR and CHA, is performed

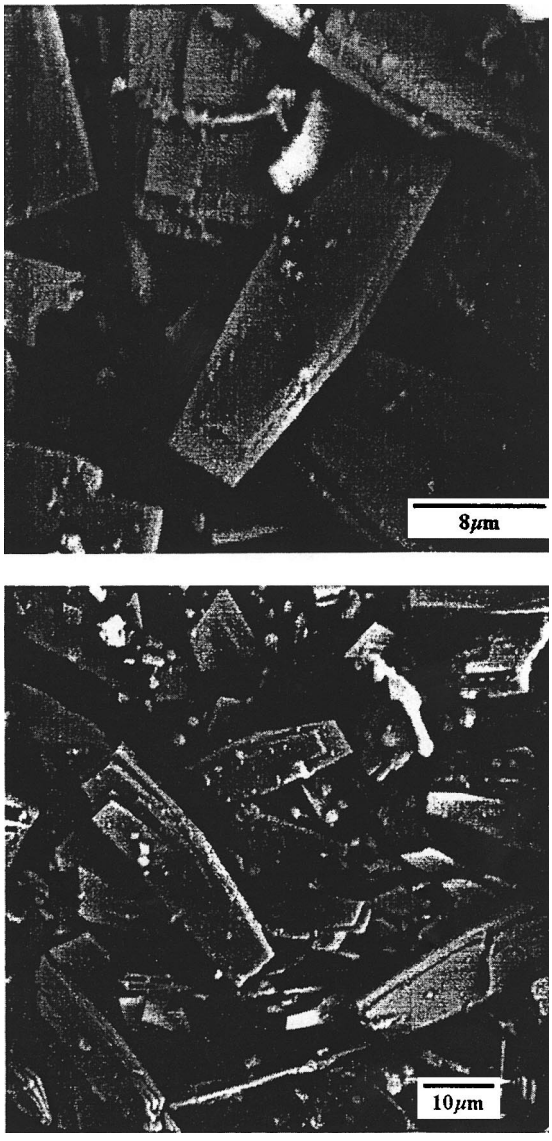

Fig. 1. Scanning Electron Microscopy (SEM) pictures of the ortho-rhombic [Fe]-CIT-5 crystals.

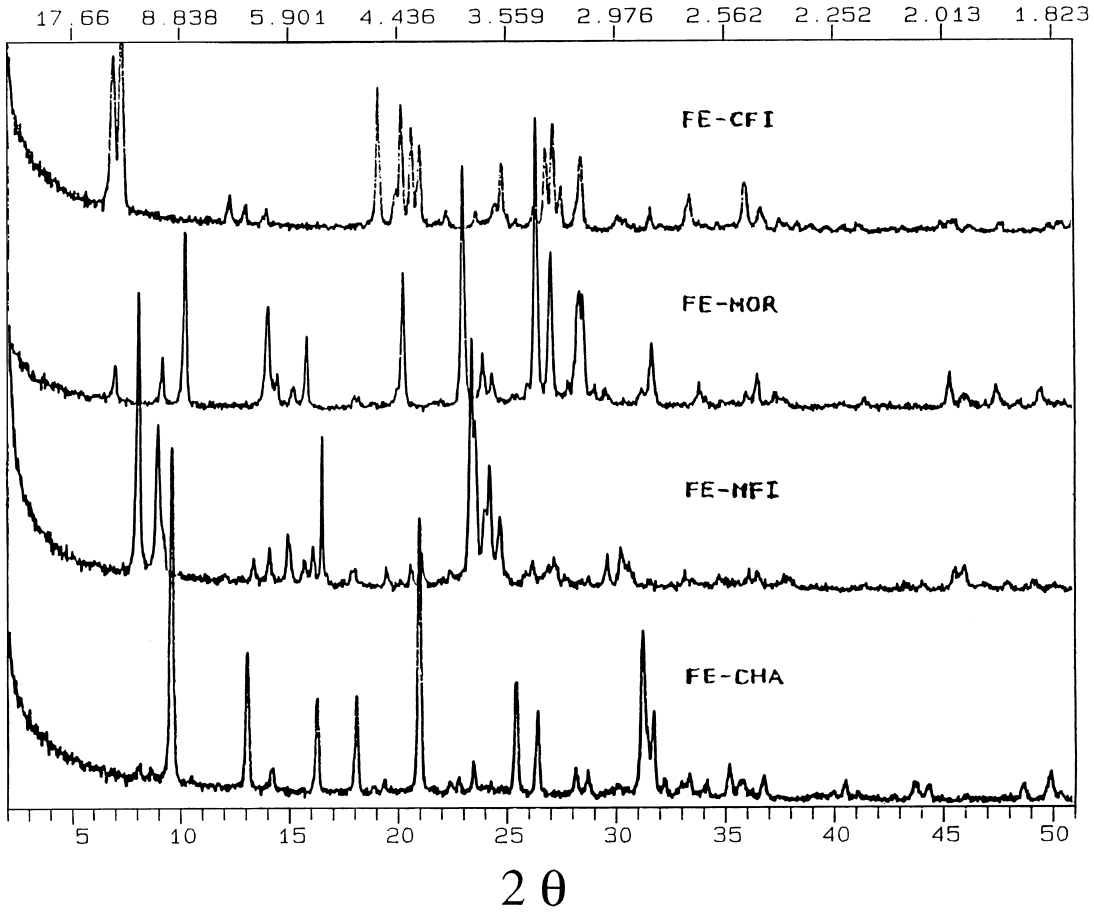

Fig. 2. X-Ray diffraction patterns of Fe-CIT-5, Fe-MOR, Fe-ZSM-5 and Fe-CHA.

via direct synthesis and post-synthetic modification. The nature of the active sites in the zeolite samples was investigated using a variety of techniques: XRD, Mossbauer spectroscopy, SQUID, EPR, DRS and Fe–K edge X-ray absorption spectroscopy. [Fe]-CIT-5 (CFI, Si/Fe $\sim$ 25) (a new 14 MR ring zeolite structure), with channel diameters of about 10.0 $\times$ 9.9 Å at intersections, has iron exclusively inside of the lattice after synthesis. For comparative reasons a second sample of Fe-CIT-5 was prepared by impregnating an aluminum CIT-5 (Si/Al $\sim$ 10) with an $Fe(acac)_2$ solution and calcined to achieve a 5 wt.% loading. Extra-framework small clusters of α-Fe_2O_3 are seen. The SEM, in Fig. 1 shows the characteristic thin flat plate orthorhombic Fe-CIT-5 crystals. The XRD data, in Fig. 2 reveal that all materials are highly crystalline. The EPR data, in Fig. 3 show the presence of tetrahedral Fe^{3+} coordination in the lattice for [Fe]-CIT-5. Thus, for [Fe]-CIT-5, [Fe]-MOR, [Fe]-ZSM-5 and [Fe]-CHA tetrahedral Fe^{3+} coordination in the lattice is observed and different (distorted) octahedral signals in the impregnated Fe-CIT-5, Fe-MOR, Fe-ZSM-5 and Fe-CHA materials are seen. In Mossbauer spectroscopy the absence and presence of a hyperfine magnetic field (HMF) for [Fe]-CIT-5 and Fe-CIT-5 are seen. EPR analysis demonstrates that the ratio of framework to non-framework iron depends on the initial framework Fe concentration of the precalcined material. When iron concentrations are kept low only framework iron is seen (below 2%). Extra-framework

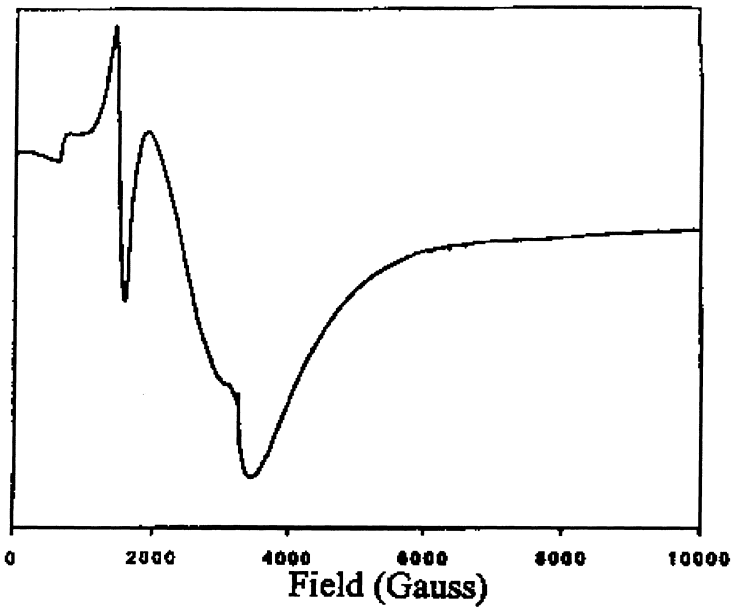

Fig. 3. Electron Paramagnetic Resonance Signal in X-band at g = 4.3 of tetrahedral Fe^{3+} coordination in the lattice of the [Fe]-CIT-5.

iron oxides are occluded by calcination of framework iron zeolites with high iron loading or physical mixtures of the aluminum containing zeolites with iron salts. When the latter procedure is applied on framework iron zeolites, extra-framework iron oxide clusters can be anchored to framework iron sites. From DRS the Al-containing samples show the strongest migration in and out of the lattice of iron upon thermal treatment. From Squid data as can be seen in Fig. 6, the magnetic character reveals paramagnetic and anti-ferromagnetic contributions. SQUID measurements show at 260 K the absence of a clear Morin transition (weak ferromagnetism as seen for the bulk iron oxide) for the Fe-ZSM-5 crystals. A paramagnetic contribution occurs from isolated iron ions (in the lattice) and an anti-ferromagnetic contribution occurs from small clusters, respectively. Shape-selective formation of nano-clusters of iron oxides with various sizes is realized inside the pore-sizes varying from 10.0 to 8.0 and 6.3 to 4.3 Å of the CFI, MOR, MFI, and CHA zeolites. The larger channels of the former two zeolites may accommodate larger iron oxide clusters within the intra-crystalline structures, and allow bi-molecular methane reactions, the latter two zeolites allow small oligo-nuclear iron clusters to be formed within the intra-crystalline structures and only allow mono-molecular methane reaction.

3.2. EXAFS Characterization

The Fe–K edge X-ray absorption data were obtained for the zeolites containing iron clusters $Fe_{5.0}$-CIT-5, $Fe_{5.0}$-ZSM-5, $Fe_{4.0}$-MOR and $Fe_{5.0}$-CHA. EXAFS X-ray absorption spectra at the Fe–K edge were collected in transmission mode using a Si(2 2 0) crystal for the mono-chromator at the Stanford Synchrotron Radiation Laboratory. The samples are diluted in a 5:2 BN:catalyst ratio to ascertain correct optical thickness of the catalyst samples. Spectra are obtained at liquid nitrogen temperature under vacuum. The reference chamber contains an iron foil, which is scanned in transmission mode at room temperature. The X-ray absorption data show the EXAFS and XANES region. The X-ray absorption data in the XANES region, the unweighted χ versus k-plots (3.5–15.86 $Å^{-1}$) and k^3 weighted uncorrected Fourrier transforms of the data are obtained. The edge shift for the Fe occurs at 7111.2 eV and increases with +14.7 eV for Fe-ZSM-5, with 15.3 eV for Fe-CIT-5 and Fe-CHA and with +15.5 eV for Fe-MOR (standard deviation

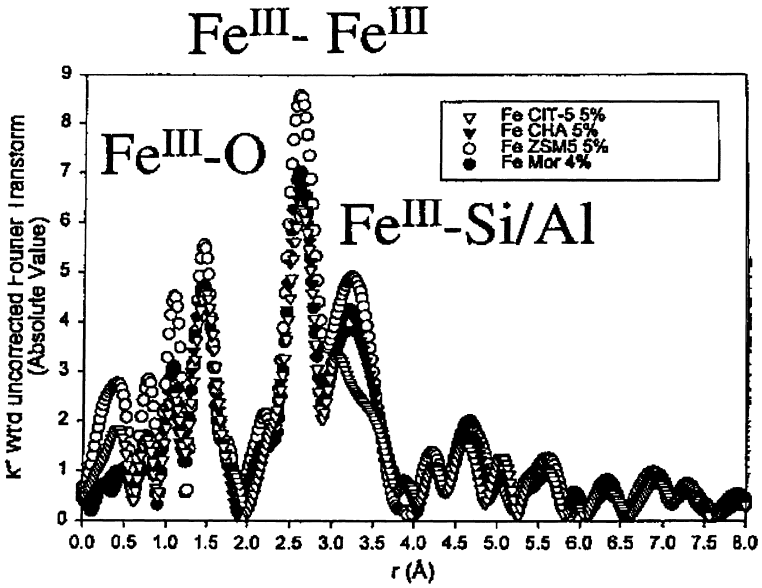

Fig. 4. EXAFS B.k^3-weighted fourier transforms of Fe-CHA, Fe-ZSM-5, Fe-MOR, Fe-CIT-5.

in the order of 0.5 eV). Since the energy resolution for the crystal, the slit size and the beam-line geometry is 3 eV these values are the same within the experimental error. In the XANES region a notable preedge feature of Fe^{3+} is seen. This feature is quite analogous to the Fe_2O_3 signature observed. The coordination geometry, i.e. for a tetrahedral cluster the t_2 orbital (3d derived) is mostly p-like and the white line at the edge in the region of the 1s εd dipole forbidden transition is seen. In the octahedral cluster this white line is practically not observed. A second shoulder can be assigned to the treshold of the 1s εp dipole allowed transitions. In Fig. 4 the EXAFS structural parameters obtained as the k^3 weighted uncorrected FT intensities as function of the distance (r, Å) can be seen. These plots are used to inverse Fourier transform the data and subsequent curve-fitting of the different peaks is performed to obtain corrected distances. The data is analyzed using XAMath, a package for reduction of XAS spectra. EXAFS data are analyzed using theoretical phase shifts and scattering amplitudes from FEFF 3.25. For iron in zeolites we use the phase and amplitude parameters of Fe_2O_3. Curve-fitting of the inverse transformed data gives an Fe–O distance of 1.7 Å in the r-window of 1.5–2.0 Å and an Fe–Fe distance of 2.7 Å in the r-window of 2.0–3.0 Å. The inverse transformed data in the r-window of 3.0–4.0 Å gives Fe–Si distances from 3.1 to 3.5 Å for CIT-5 and around 3.3 Å for CHA, ZSM-5 and MOR with a high Debye–Waller factor (0.0060 $Å^2$). For Fe-CIT-5 the shell of Si and Al shows the biggest deviation in distances due to the side pockets in the 10 Å linear channels, so iron oxide clusters exist in either the 10 or 12 Å cages.

3.3. QM/MM Characterization

The ab initio calculations used involve full geometry optimization of the clusters with density functional theory (dft) [28,29] as implemented in Jaguar (Jaguar 3.0, Schrodinger Inc., Portland, Oregon, 1997) at the B3LYP method level (Becke3 hybridization functionals, Slater/Becke88 non-local exchange and Li, Yang, Parr local and non-local correlation corrections to the local potential energy functionals of Vosko, Wilk and Nusair) using the Los Alamos effective core potential and valence double zeta for iron (LACVP** basis sets). The molecular mechanics calculations involve a new molecular mechanics force field, the universal force field (UFF) of Rappé et al. [30,31]. The force field parameters are estimated using general rules based only on the element, its hybridization and its

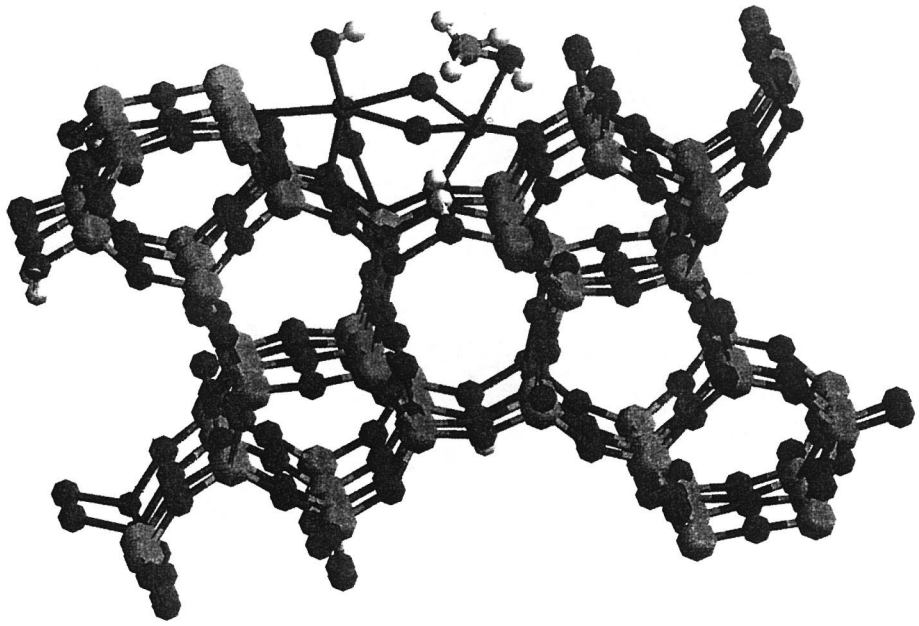

Fig. 5. QM-MM analysis of the di-nuclear [(Fe-ZSM-5)$Fe_2(H–O)_2(OH)(OHCH_3)$] structure in which a di-nuclear cluster within the channel is linked to the iron ZSM-5 lattice via O coordination.

connectivity. The force field functional forms, parameters, and generating formulas for the full periodic table have been published [30]. For charge equilibration used in molecular dynamics simulations the charges in the complexes were determined [31]. This helps to readjust charges based on geometry and experimental properties. In di-nuclear iron complexes the Fe–O bond distances measure between 1.92 and 1.94 Å as obtained from QM for the bonds in the direction of the equatorial unprotonated and protonated O groups. The Fe-O bonds are accompanied by Fe–O–Fe angles close to the 90–93° and to a O–Fe–O bite angle of 74.5°. In these cases the iron is 5 or 6 (O_h) coordinated [30–33]. In mono-nuclear iron complexes the Fe–O bond distances of 1.86 Å (2+, O_h) 6 coordinated and 1.90 Å (3+, T_d) 4 coordinated. For tetrahedral iron and silicon atoms bond distances of 1.65 for Si–O and 1.90 Å for Fe–O obtained from QM seen in the direction of the Fe–O–Si bridge, are accompanied by Fe–O–Si angles close to the 131.2° and to a O–Fe–O bite angle of 109.47°. In QM the order of the angles is such that Fe–O–Si(Al) > O–Fe *tetr*-O > Fe–O–Fe > O–Fe *oct*-O, in particular the first value is much higher in QM compared to UFF and the last value is much lower in QM compared to UFF. The framework structure of Fe-ZSM-5, with bridging oxygen atoms present as dark spheres and silicon atoms present as light spheres, is shown in Fig. 5 with a view down the 10 MR pores, at which a di-nuclear iron site is anchored to the surface. In Fig. 6 the average magnetic susceptibility is shown in a χT versus T-plot. The anti-ferromagnetic coupling is seen for Fe-ZSM-5 (A) and Fe-CIT-5 (B) samples as on cooling χT decreases which indicates that the excited undecuplet state is depopulated in favor of the non-uplet ground state. The framework structure of Fe-CIT-5 (C), with bridging oxygen atoms omitted, is shown in Fig. 7 with a view down the 14 MR pores, as is the SDA *N*(16)-methyl-sparteinium-hydroxide (**I**).

3.4. Formation of α-oxygen sites

The as-synthesised [Fe]-CHA, [Fe]-ZSM-5, [Fe]-MOR and [Fe]-CIT-5 samples are calcined under N_2 to 175°C for 2 h, then heated at 550°C for 5 h, 1 h in a N_2 atmosphere and consecutively in air for 4 h. The Fe-CHA, Fe-AlZSM-5, Fe-MOR or Fe-HAlCIT-5 are calcined under N_2 to 175°C, re-

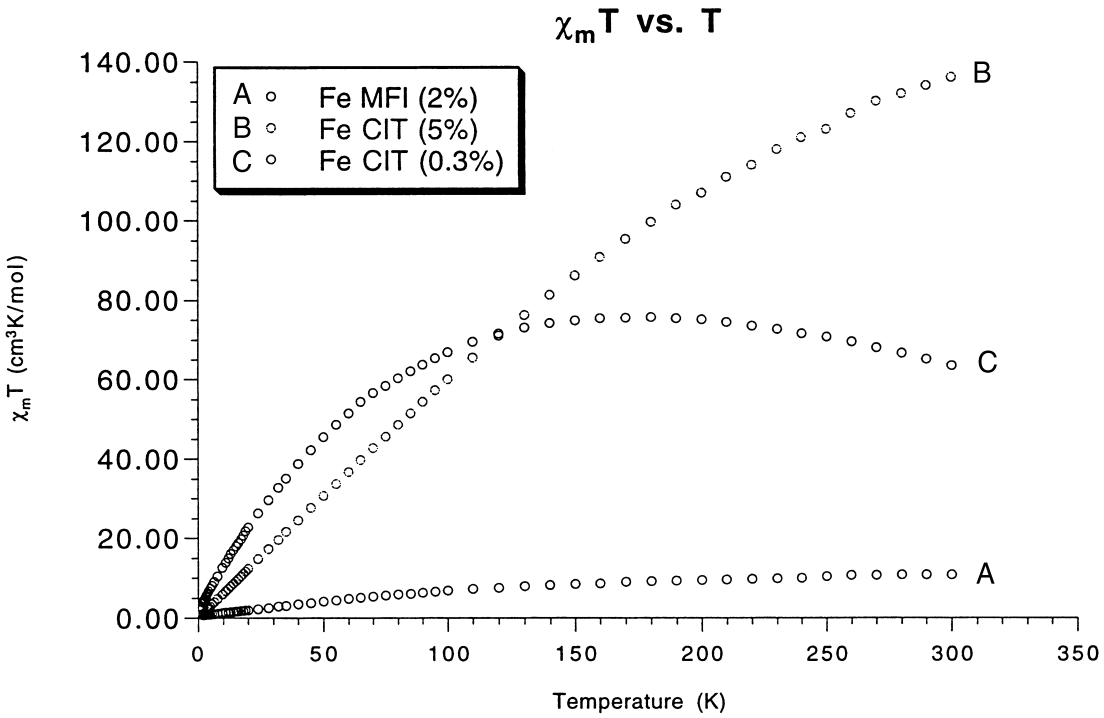

Fig. 6. The product of the Magnetic susceptibility and temperature χT as a function of temperature T for iron in three different catalyst preparations, (A) lattice iron in [Fe]-ZSM-5, (B) iron dispersed by solid state exchange in Fe-CIT-5 and (C) lattice iron in [Fe]-CIT-5.

main at 175°C for 2 h, is then heated under N_2 to 550°C in 5 h, remains at 550°C for 1 h and then in air for 4 h to produce the acid form. The zeolites are then evacuated for 2–12 h at 550–800°C. After cooling they are treated with N_2O at 250°C for 1–2 h at relatively low pressures (below 250 Torr), adsorption of N_2O at higher temperatures, e.g. 550°C results in the formation of molecular oxygen. After treatment with N_2O the catalyst is subjected to a vacuum of 10^{-3} atm for a variable time (10 min) to remove the nitrogen and unreacted N_2O from the quartz cell and is then cooled down to 20°C.

3.5. Conversion of methane to methanol

After N_2O treatment, the catalyst is reacted with methane at 20°C for a variable time (10 min to 4 h) and then extracted with a variety of solutions, e.g. acetonitrile-water or pure water H_2O or D_2O. ^{1}H NMR evaluation reveals the presence of methanol (chemical shifts around 3 ppm) in the liquid. Methanol in liquid and bound on Al-sites in zeolites are characterized respectively, by chemical shifts of 49 and 54 ppm in ^{13}C NMR. Solid state ^{27}Al MAS-NMR analysis of the methanol loaded catalyst shows the occurrence of the tetrahedral Al at 54.35 ppm with a full width at half maximum (FWHM) of 596 Hz and a very small signal of octahedral Al around 0 ppm (−0.7 ppm). After the catalytic reaction the broadened signal with a FWHM of 1680 Hz at 54.48 ppm shows a strongly decreased intensity. The occurrence of a small shoulder at 44 ppm is right at the edge of the region assigned to penta-coordinated Al species (26–44 ppm). Due to the interaction of methanol with quadrupolar nuclei, a broadening and decrease of signal intensity occurs. The parameters that affect the catalytic results are the size of the iron clusters, which are function of the zeolite crystallite size (smaller crystals give better dispersions and smaller iron clusters), the various Si/Al ratios, the amount of iron in the sample and the pretreatment conditions.

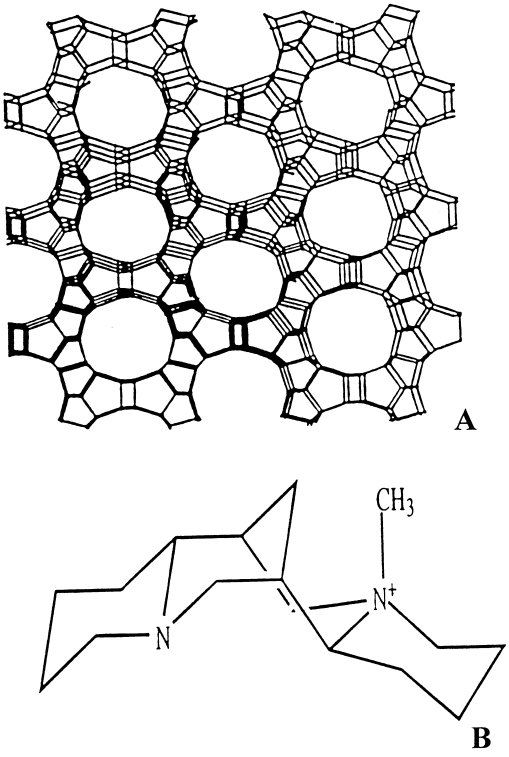

Fig. 7. Zeolite framework structure of Fe-CIT-5 and it's organic structure directing agent, *N*(16)-methyl-sparteinium-hydroxide (**I**) (MeSPAOH).

In a study of the reactivity of the tetrahedral Fe^{3+} coordination in the lattice for [Fe]-CIT-5, [Fe]-MOR, [Fe]-ZSM-5 and [Fe]-CHA, none of the pretreatment or activation effects, helped the reaction of methane to methanol, thus, mono-nuclear iron sites are not active in this reaction. In order to study the pretreatment effects, the Fe_x-ZEO samples are pretreated with O_2 at 550°C, then under vacuum under a variety of temperatures: 550, 750, 800, 900°C. Extraction with water shows quantities of methanol dependent on the activation technique; no methanol was observed at 55°C, a moderate yield of 28 mmol at 750°C, a similar yield of 163 mmol at 800 and 900°C. Thus, in further experiments we chose the evacuation at 800°C.

In a second series of experiments, the activation effects are probed. We use a pretreatment under O_2 at 550°C and a sample evacuation at 800°C. Activation in absence of oxidant (blank control 1) uses a pretreatment of the Fe-ZSM-5 to 900°C and then allows to cool to 20°C, always under O_2. After purging and reaction with CH_4 at 20°C and H_2O extraction no methanol is observed. In absence of thermal activation (blank control 2) no products are observed either. The reduction of Fe^{3+} to Fe^{2+} is claimed [1] as a requisite to the formation of methanol.

In a third series of experiments, the effects of zeolite structure and loading of Fe are evaluated. Pretreatment is performed by evacuation at 800°C, activation with N_2O at 250°C and reaction with CH_4 occurs at 20°C. Extraction and quantification are similar as for series 1, for the highest yield case, methanol can be observed and quantified by ^{1}H NMR of the solution. Catalysis with the Fe-ZSM-5 (Si/Al ratio 11) at different iron loading gives different results.

As can be seen in Table 1 $Fe_{0.5}$-ZSM5 shows no activity, whereas $Fe_{2.0}$-ZSM5 shows 97.2 μmol CH_3OH/g catalyst and $Fe_{5.0}$-ZSM5 shows 163 μmol CH_3OH/g catalyst. Analysis of 1 g of $Fe_{2.0}$-ZSM5 contains 20 mg Fe or 364 μmol Fe/g catalyst. Catalysis with the 5 wt.% Fe loaded samples of Fe-CIT-5, Fe-MOR, Fe-ZSM-5 and Fe-CHA gives 76, 92, 163 and 10 μmol methane oxidation products, respectively. The first two catalysts also give only between 5 and 10% methanol and 30 and 40% of various (oxygenated) coupling products, as other non-selective products are formed. Di-deuteromethane and $^{13}CH_4$ oxidation [1–3] with α-oxygen suggest that the oxidation involves a rate determining C–H bond cleavage with high KIE (KIE = kH/kD). Regeneration experiments show that multiple use of the catalyst in several cycles of this process occur with a limited decay in activity of about 20%. To conclude from the preceding results, the $Fe_{5.0}$-ZSM-5 is the best zeolite, the [Fe]-ZSM-5 is inactive. The $Fe_{5.0}$-CIT-5 gives various products, the selectivity for methanol is inferior, the [Fe]-CIT-5 is again inactive. All silica systems are inactive, metal-oxide and support increase the activity. Thus, mono-nuclear tetrahedral iron sites in the lattice remain inactive, the same is true for large particles of an oxide dispersed phase at the outer surface of zeolites, whereas small complexes (bi- or oligo-nuclear) in the intra-crystalline space of zeolites formed by dispersion of iron oxide prove most active.

Table 1
Partial oxidation of methane with α-Fe sites in ZSM-5 and other Zeolites[a]

Zeolite	% Fe	Oxidation	μmol Fe	μmol MeOH
ZSM-5 Si/Al 11	0.5%	5 Torr N_2O/250°C	75	–
ZSM-5 Si/Al 11	2.0%	5 Torr N_2O/250°C	360	97
ZSM-5 Si/Al recycle	2.0%*	5 Torr N_2O/250°C	360	76
ZSM-5 Si/Al 11	5.0%	5 Torr N_2O/250°C	800	163
ZSM-5 Si/Al 11	5.0%	10 Torr N_2O/250°C**	800	208
ZSM-5 Si/Al 11	5.0%	10 Torr N_2O/250°C/CD_2H_2/20°C**	800	186
ZSM-5 Si/Al 81	5.0%	5 Torr N_2O/250°C	800	49
ZSM-5 Si/Al 81	5.0%	5 Torr O_2/550°C	800	< 1
ZSM-5 Si/Al 81	5.0%	5 Torr O_2/800°C	800	< 1
CHA (0.1 μm)	5.0%	5 Torr N_2O/250°C	800	10 (10)
MOR (1–3 μm)	5.0%	5 Torr N_2O/250°C	800	10 (33)***
CIT (3–7 μm)	5.0%	5 Torr N_2O/250°C	800	4 (39)***

[a] In all experiments the Fe-Zeolite catalyst was used, 5 Torr N_2O is equilibrated on the catalyst for 2 hours at 250°C and 5 Torr CH_4 is equilibrated on the catalyst for 1 to 2 hours at 20°C.

* Catalyst is recycled by calcination at 550°C and evacuation at 900°C.

** Equilibration pressures increases to +−10 Torr N_2O, +−10 Torr CH_4.

*** Methanol and various (oxygenated) coupling products were formed.

4. Conclusions

Mono-nuclear iron sites in [Fe]-ZSM-5, di-nuclear iron clusters stabilized inside the matrix of thermally activated Fe-ZSM-5 and iron sites associated with nano-hematite phases in ZSM-5 and various other zeolites are compared using theoretical tools as well as experiments. For [Fe]-CIT-5, [Fe]-MOR, [Fe]-ZSM-5 and [Fe]-CHA tetrahedral Fe^{3+} coordination in the lattice is observed by EPR and different (distorted) octahedral signals in the impregnated Fe-CIT-5, Fe-MOR, Fe-ZSM-5 and Fe-CHA materials are seen. EXAFS data on highly loaded samples with 5 wt.% iron gives an Fe–O distance of 1.7 Å and an Fe–Fe distance of 2.7 Å in and Fe–Si distances from 3.1 to 3.5 Å for CIT-5 and around 3.3 Å for CHA, ZSM-5 and MOR. For tetrahedral iron and silicon atoms bond distances of 1.65 for Si–O and 1.90 Å for Fe–O as obtained from QM, in the direction of the Fe–O–Si bridge, the Fe–O–Si angles are close to 131.2°. For the di-nuclear iron complexes bond distances of 1.95 and 1.99 Å obtained from QM, in the direction of the Fe–O groups, accompanied by Fe–O–Fe angles close to 90–93° and an O–Fe–O bite angle of 74.5°. Methane can be converted into methanol with α-oxygen at room temperature using N_2O as a selective oxidant inside the pores of various zeolites. Extraction of the catalysts with water is preferred over acetonitrile-water mixtures. The iron oxide clusters realize the sub-stoichiometric oxidation of methane, favoring oxygen insertion chemistry over coupling chemistry. Whereas the [Fe]-ZSM-5 and the [Fe]-CIT-5 are inactive, $Fe_{2.0}$-ZSM-5 and $Fe_{5.0}$-ZSM-5 are the best zeolites, indicating the necessity of an iron loading >0.5 wt.% Fe to observe methanol formation. $Fe_{5.0}$-CIT-5 gives various products, the selectivity for methanol is lower, other products are also seen, due to absence of product shape-selective containment.

Acknowledgements

PPKG thanks NATO for a post-doctoral position at the Beckman Institute, CalTech and FWO-Flanders for a fellowship as post-doctoral scholar at the K.U. Leuven. PPKG thanks Prof. M.E. Davis and Dr. J. Labinger for discussions and BP Amoco Chemical Inc., for financial support. We also wish to thank Dr. J. Goellner and Prof. B.C. Gates of U.C. Davis for taking the XAFS spectra and discussions of the data.

References

[1] G.I. Panov, V.I. Sobolev, K.A. Dubkov, A.E. Parmon, N.S. Ovanyesan, A.E. Shilov, A.A. Shteinman, React. Kinet. Catal. Lett. 61 (1997) 251.

[2] K.A. Dubkov, V.I. Sobolev, G.I. Panov, Kinet. Catal. 39 (1998) 72–299.
[3] N.S. Ovanyesan, A.A. Shteinman, K.A. Dubkov, V.I. Sobolev, G.I. Panov, Kinet. Catal. 39 (1998) 792.
[4] G.I. Panov, V.I. Sobolev, A.S. Kharitonov, J. Mol. Catal. 61 (1990) 85.
[5] V.I. Sobolev, G.I. Panov, A.S. Kharitonov, A.M. Volodin, V.N. Romanikov, K.G. Ione, J. Catal. A 139 (1993) 435.
[6] P. Wagner, M. Yoshikawa, M. Lovallo, K. Tsuji, M. Tsapatsis, M.E. Davis, J. Chem. Soc., Chem. Commun. 22 (1997) 2179.
[7] T. Ito, J.H. Lunsford, Nature 314 (1985) 721.
[8] J.S.J. Hargreaves, G.J. Hutchings, R.W. Joyner, Nature 348 (1990) 428.
[9] J.R. Anderson, P. Tsai, J. Chem. Soc., Chem. Commun. 1435 (1987).
[10] R. Shah, M.C. Payne, J.D. Gale, Science 271 (1996) 1395.
[11] J. Cejka, A. Vondrova, B. Wichterlova, G. Vorbeck, R. Fricke, Zeolites 14 (1994) 147.
[12] Y.F. Chang, J.G. McCarty, Y.L. Zhang, Catal. Lett. 34 (1995) 163.
[13] X.B. Feng, W.K. Hall, J. Catal. 166 (1997) 368.
[14] A.S. Kharitonov, G.I. Panov, K.G. Ione, V.N. Romanikov, G.A. Sheveleva, L.A. Vostrovikova, V.I. Sobolev, US Patent 5,110,995 (1992).
[15] G.I. Panov, A.S. Kharitonov, G.A. Sheveleva, WO 95/27691 (1994).
[16] V.I. Sobolev, K.A. Dubkov, O.V. Panna, G.I. Panov, Catal. Today 24 (1995) 251.
[17] K.A. Dubkov, V.I. Sobolev, E.P. Talsi, M.A. Rodkin, N.H. Watkins, J. Mol. Catal. A 123 (1997) 155.
[18] V.I. Sobolev, K.A. Dubkov, E.A. Paukshtis, L.V. Pirutko, M.A. Rodkin, G.I. Panov, Appl. Catal. A 141 (1996) 185.
[19] G.I. Panov, V.I. Sobolev, K.A. Dubkov, A.S. Kharitonov, Stud. Surf. Sci. Catal. 101 (1996) 493.
[20] A.K. Uriarte, M.A. Rodkin, M.J. Gross, A.S. Kharitonov, G.I. Panov, Stud. Surf. Sci. Catal. 110 (1997) 857.
[21] G.I. Panov, A.K. Uriarte, M.A. Rodkin, V.I. Sobolev, Catal. Today 41 (1998) 365.
[22] M. Hafele, A. Reitzmann, E. Klemm, G. Emig, Stud. Surf. Sci. Catal. 110 (1997) 847.
[23] E. Suzuki, K. Nakashiro, Y. Ono, Chem. Lett. 953 (1988).
[24] Y. Ono, K. Tohmori, S. Suzuki, K. Nakashiro, E. Suzuki, Stud. Surf. Sci. Catal. 41 (1988) 75.
[25] M.H. Gubelmann, P.J. Tirel, EP 341165 (1989).
[26] M.H. Gubelmann, J.M. Popa, P.J. Tirel, EP 406050 (1990).
[27] P.J. Tirel, M.H. Gubelmann, J.M. Popa, in: Proceedings of the 9th International Zeolites Conference, Rec. Prog. Rep., Montreal.
[28] R.H. Crabtree, Chem. Rev. 95 (1995) 987.
[29] P.E. Siegbahn, R.H. Crabtree, J. Am. Chem. Soc. 119 (1997) 3103.
[30] A.K. Rappe, C.J. Casewit, K.S. Colwell, W.A. Goddard, W.M. Skiff, J. Am. Chem. Soc. 114 (1992) 10024.
[31] A.K. Rappe, W.A. Goddard, J. Chem. Phys. 95 (1991) 3358.
[32] P.P. Knops-Gerrits, A. Weiss, S. Dick, P.A. Jacobs, Stud. Surf. Sci. Catal. 110 (1997) 1061.
[33] P.P. Knops-Gerrits, A.M. Van Bavel, G. Langouche, P.A. Jacobs, in: Derouane, et al. (Eds.), NATO ASI Proceedings, 1998, pp. 3.44, 215.
[34] P.P. Knops-Gerrits, A. Verberckmoes, R.A. Schoonheydt, M. Ichikawa, P.A. Jacobs, Microporous Mesoporous Mater. 21 (4–6) (1998) 475.